

# Modelling thermal conductivity and collective effects in a simple nanofluid

Mihail Vladkov <sup>\*</sup>, Jean-Louis Barrat <sup>†1</sup>

<sup>1</sup> *Laboratoire de Physique de la Matière Condensée et Nanostructures Université Lyon 1; CNRS; UMR 5586 Domaine Scientifique de la Doua F-69622 Villeurbanne cedex; France*

(Dated: July 11, 2021)

## Abstract

Molecular dynamics simulations are used to model the thermal properties of a fluid containing solid nanoparticles (nanofluid). The flexibility of molecular simulation allows us to consider the effects of particle mass, particle-particle and particle-fluid interaction and that of the spatial distribution of the particles on the thermal conductivity. We show that the heat conductivity of a well dispersed nanofluid is well described by the classical Maxwell Garnett equation model. In the case of particle clustering and strong inter particle interactions the conductivity can be again described by effective medium calculation taking into account the aspect ratio of the cluster. Heat transfer is increased when particles are aligned in the direction of the temperature gradient. This kind of collective effects could be a first step to understand the substantial increase in the conductivity observed in some experiments.

---

<sup>\*</sup> E-mail: mihail.vladkov@lpmcn.univ-lyon1.fr

<sup>†</sup> E-mail: jean-louis.barrat@lpmcn.univ-lyon1.fr

Many experimental studies have suggested that the thermal conductivity of colloidal suspensions referred to as “nanofluids” is unusually high<sup>1,2</sup>. Predictions of effective medium theories are accurate in some cases<sup>3</sup> but generally fail to account for the large enhancement in conductivity. In spite of a large number of - sometimes conflicting or controversial - suggestions and experimental findings<sup>4</sup>, the microscopic mechanisms for such an increase remain unclear. One of the possibilities that was suggested was the effect of Brownian motion<sup>5</sup>, and appeared to be an attractive and generic explanation. The essential idea is that the Brownian velocity of the suspended particle induces a fluctuating hydrodynamic flow<sup>6,7</sup>, which on average influences (increases) thermal transport. This mechanism is different from transport of heat through center of mass diffusion, the contribution of which was previously shown to be negligible<sup>8</sup>. However, some recent experimental high precision studies reported a normal conductivity in nanoparticle suspensions at very small volume fractions below 1%<sup>9</sup>, questioning the validity of this assumption. Recent simulations also showed that normal conductivity is expected for low volume fractions (around 3.3%)<sup>11</sup> as well as for volume fractions up to 13%<sup>10</sup> establishing that the physical parameter determining thermal properties should be the particle interfacial thermal resistance.

We also recently established by simulations that Brownian motion and Brownian velocity field have no effect on the heat transfer of a single nanoscopic particle with the surrounding fluid<sup>10</sup>. Thus the explanation of the increase in conductivity is currently to be looked for mostly in some collective effects between particles - a field that has not been studied through microscopic simulation.

In this work we use non equilibrium molecular dynamics “experiments” to explore further the transfer of heat in a model fluid containing nanoparticles. We make use of the flexibility allowed by molecular simulations to explore extreme cases in terms e.g. particle/fluid mass density mismatch. We concentrate on model systems that are expected to be representative of generic properties. We explore a large range of parameters and make a quantitative comparison with effective medium calculations. By studying the thermal conductivity in a system with two particles and by precisely controlling their positions we are able to observe the influence of collective effects consisting in different

particle-particle interactions and displacement with respect to the temperature gradient.

We start by describing our simulation methodology and presenting results about the conductivity of a fluid containing a single nanoparticle in a temperature gradient. We then study the conductivity of a system containing two particles varying their positions and the intensity of their interactions.

## I. SIMULATION METHOD

The model fluid used in this study is a simple Lennard-Jones liquid. The nanoparticles (solid phase) are obtained by a spherical cut of a bulk FCC crystal. All atoms in our system interact through Lennard-Jones interactions

$$U_{ij}(r) = \begin{cases} 4\varepsilon((\sigma/r)^{12} - c(\sigma/r)^6), & r \leq r_c \\ 0, & r > r_c \end{cases} \quad (1)$$

where  $r_c = 2.5\sigma$ . The coefficient  $c$  is equal to 1 for atoms belonging to the same phase, but can be adjusted to modify the wetting properties of the liquid on the solid particle<sup>12,13</sup>. A coefficient of  $c = 1$  defines a wetting interaction while the non wetting case is modelled by  $c = 0.5$ . Within the solid particles, atoms are linked with their neighbors through a FENE (Finite extension non-linear elastic) bonding potential:

$$U_{FENE}(r) = \frac{k}{2}R_0 \ln(1 - (\frac{r}{R_0})^2), \quad r < R_0 \quad (2)$$

where  $R_0 = 1.5\sigma$  and  $k = 30.0\varepsilon/\sigma^2$ . This potential, combined with the Lennard-Jones interaction results in a narrow distribution of the distance between linked atoms around  $0.97\sigma$ . A solid particle in the fluid was prepared as follows: starting from a FCC bulk arrangement of atoms at zero temperature, the atoms within a sphere were linked to their first neighbors by the FENE bond. Then the system was equilibrated in a constant NVE ensemble with energy value corresponding to a temperature  $T = 1$ . A particle contains 555 atoms, surrounded by the atoms of the liquid. The number density in the system is  $\rho = 0.85\sigma^{-3}$ . As the simulated particles are not exactly spherical, but present some FCC facets, their radius was estimated from the radius of gyration:

$$\langle R_g^2 \rangle = \frac{1}{N} \sum_1^N (r_i - r_{CM})^2 = \frac{3}{5}R_p^2 \quad (3)$$

where  $R_g^2$  is the measured radius of gyration of the particle atoms, and the second equality applies to an ideal sphere. Taking  $\sigma = 0.3nm$  this corresponds to a particle radius of order  $R_{part} \sim 1.5nm$ . The solid particles obtained by this procedure behave very closely as ideal harmonic solids. Non linear effects associated with the non linearity of the bonding potential are absent in a wide temperature range. This assumption was verified through equilibrium simulations at different temperatures, monitoring the energy per particle. The observed relation is linear and indicates a particle heat capacity very close to  $3k_B T N$ , as for an harmonic ideal solid, in a temperature range from  $T = 1$  to  $T = 3.5$ . We study systems of wetting ("hydrophilic",  $c = 1$ ) and non wetting ("hydrophobic"  $c = 0.5$ ) particles, different values of the density mismatch between the solid and liquid phase ( $m_p/m_l = 1, 50, 100$  where  $m_l$  is the mass of a fluid atom and  $m_p$  is the mass of a particle atom) and different particle volume fractions.

### A. Simulating Heat Flow and Measuring Conductivity

The most simple and direct method of measuring thermal conductivities in a simulation is undoubtedly non equilibrium molecular dynamics. With this set up a temperature gradient is established through the sample and thermal properties are calculated from the measurement of energy fluxes. This method involves locally injecting and evacuating heat in the system. In our study this is achieved by applying two thermostats with different temperatures in the two ends of a fluid slab. The periodicity of the box is maintained in the directions perpendicular to the temperature gradient and the system is non periodic in the direction of the heat flux. If one allows the gradient to change sign in the simulation box a stationary heat flow can be achieved in a fully periodic box<sup>11</sup>. However with this setup special attention should be payed in the regions of abrupt change in the temperature gradient, and the simulated system is less realistic.

The systems we study are periodic in the  $x$  and  $y$  directions. In the transverse  $z$  direction, the liquid is confined by a repulsive potential (ideal flat wall). The thermostats are applied to a fluid slice in the vicinity of the walls of width of around 3 atom diameters. The thermostat consists in a rescaling of the velocities of the particles currently present

in the slice at a given time interval. The temperature measured locally in slices parallel to the heat flow direction shows that a linear profile is established in the fluid slab. The value of the temperature gradient depends on the temperature of the thermostats and their rescaling time constant (see fig. 1).

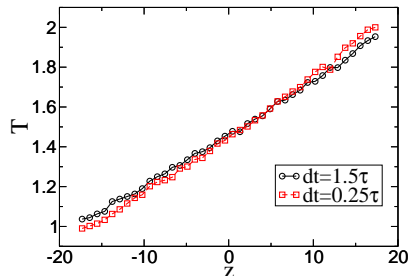


FIG. 1: Dependence of the temperature profile on the thermostat time constant for a pure liquid. A smaller rescaling interval increases the efficiency of the energy transfer between the thermostat and the liquid inducing a smaller temperature jump.

A smaller rescaling interval increases slightly the energy transfer between the thermostat and the fluid thus maintaining the thermostatted layer at an average temperature closer to the temperature of the thermostat. It is thus important to have the same time constant for the thermostat in all the systems in order to compare the values of the energy flow and detect its variations in the different setups. We set this value to  $dt = 1.5\tau$  in the simulations. Using this heat transfer setup, the local thermal conductivity is given by:

$$\lambda(z) = \frac{J(z)}{\nabla T(z)} \quad (4)$$

where  $J(z)$  is the heat flow and  $T(z)$  the temperature. This formula is easily generalized to the whole slab by taking the heat flow at the thermostats and a mean slope of the temperature profile. The problem is that such an estimation of the mean gradient is prone to error. The mean temperature profile for a pure liquid has a well defined slope, even if the fluctuations and the fitting procedure cause error. The situation is worse in the presence of nanoparticles. The temperature profile averaged over liquid and solid atoms has noticeable fluctuations around the particles as the gradient is different in the

two phases. That is why measuring an effective value of the conductivity that does not involve fitting and assuming linear temperature profile is preferable. If the thermostat relaxation time is constant for all systems, a well defined values are the two thermostats temperatures. Thus we define the slab conductivity as:

$$\lambda_{eff} = \frac{J}{(T_1 - T_2)/L} \quad (5)$$

where  $J$  is the mean stationary heat flux measured by the thermostats,  $T_i$  is the temperature of the thermostat  $i$  and  $L$  is the length of the simulation box in the  $z$  dimension. The conductivity defined in this way is sensitive only to variations in the energy flux and is a precise method for capturing variations in conductivities between systems.

To avoid any effect of thermophoresis or coupling of the thermostat to the particle, the particles are constrained to stay away from the thermostatted regions by tethering weakly their center of mass to a fixed point by harmonic springs of stiffness  $k = 30$ . Controlling the particles position also allows us to study different configurations and explore the influence of the spatial distribution of the particles on the thermal properties. The temperatures of the two thermostats were  $T_1 = 2$  and  $T_2 = 1$ . In order to compare the conductivity results for the different systems they were first equilibrated to the same pressure at a temperature  $T = 1.5$ , then a non equilibrium run was performed for about 1500-2000  $\tau_{LJ}$  to make sure the pressure stays the same for the systems of different nature and finally a production run of about 15000  $\tau_{LJ}$  during which thermostats energy, particle positions and temperature profiles are monitored. In nanoscale systems it has been observed that interfacial effects are very important<sup>10</sup>. In order to compare quantitatively the conductivity variations to the predictions of effective medium calculations it is necessary to know the value of the interfacial (Kapitza) thermal resistance. The values used in our study were determined for different wetting and particle masses by a transient adsorption simulation as explained in ref.<sup>10</sup>. In real units, a value  $R_K = 1$  corresponds typically to an interfacial *conductance*  $G = 1/R_K$ , of the order of 100MW/Km<sup>2</sup><sup>1</sup>. We study systems

---

<sup>1</sup> The conversion to physical units is made by taking a Lennard-Jones time unit  $\tau_{LJ} = 10^{-12}s$ , and a length unit  $\sigma = 0.3nm$ . The unit for  $G$  is *energy/temperature/(length)<sup>2</sup>/time*. As the energy/temperature ratio is given by the Boltzmann constant  $k_B$ , we end up with a unit for  $G$  equal to

with particle volume fraction of 13% or 12%. The volume fraction is defined as the volume of the particle divided by the volume of the fluid outside the thermostats.

## II. RESULTS AND DISCUSSION

### A. Single Particle in a Heat Flux

First we investigate the effect of the presence of a single nanoparticle on the thermal conductivity of the fluid. In this system the center of mass of the particle is held at equal distance from the two thermostats (fig. 2).

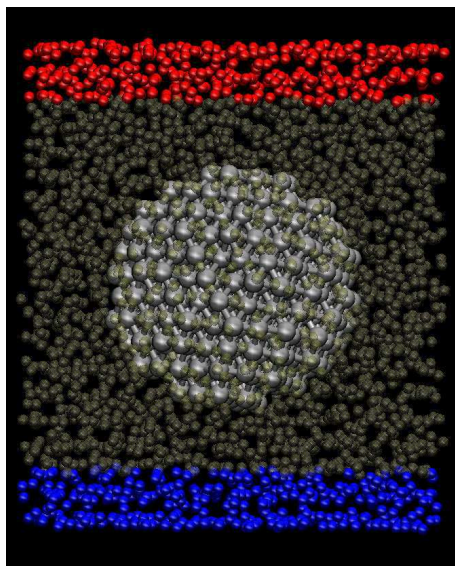


FIG. 2: Snapshot of the system used to evaluate the thermal conductivity with a particle of 13% volume fraction.

We performed simulations for a small volume fraction ( $\Phi \sim 2\%$ ), where we were not able to detect any change in thermal conductivity compared to the bulk fluid. At a higher volume fraction ( $\Phi \sim 13\%$ ), on the other hand, we observe a clear *decrease* in the heat conductivity associated with the presence of the nanoparticle (fig. 3). The Kapitza resistance  $R_K$  for the considered particles ranges from 1 to 7 so that the associated

---

$k_B/\sigma^2/\tau_{LJ} \simeq 10^8 W/m^2/s$

characteristic Kapitza length is in all cases of the order of the particles diameter. This means that the decrease must be interpreted in terms of interfacial effects. To quantify these effects, we use the Maxwell-Garnett approximation for spherical particles, modified to account account for the Kapitza resistance at the boundary between the two media. The resulting expression for the effective conductivity<sup>14</sup> (see appendix) is

$$\frac{\lambda_{eff}}{\lambda_l} = \frac{\left(\frac{\lambda_p}{\lambda_l}(1 + 2\alpha) + 2\right) + 2\Phi\left(\frac{\lambda_p}{\lambda_l}(1 - \alpha) - 1\right)}{\left(\frac{\lambda_p}{\lambda_l}(1 + 2\alpha) + 2\right) - \Phi\left(\frac{\lambda_p}{\lambda_l}(1 - \alpha) - 1\right)} \quad (6)$$

where  $\lambda_l$  and  $\lambda_p$  are the liquid and particle conductivities,  $\Phi$  is the particle volume fraction and  $\alpha = \frac{R_K \lambda_l}{R_p}$  is the ratio between the Kapitza length (equivalent thermal thickness of the interface) and the particle radius. This model predicts an increase in the effective conductivity for  $\alpha > 1$  and a decrease for  $\alpha < 1$ , regardless of the value of the conductivity of the particles or of the volume fraction. The prediction depends very weakly on the ratio  $\lambda_p/\lambda_l$ , less than 1% for  $10 < \lambda_p/\lambda_l < 100$ . The minimum value of  $\lambda_{eff}/\lambda_l$ , obtained when  $\alpha \rightarrow \infty$ , is  $\frac{1-\Phi}{1+\Phi/2}$  while the maximum possible enhancement (for  $\lambda_p \rightarrow \infty$  and  $R_K \rightarrow 0$ ) is  $\frac{1+2\Phi}{1-\Phi}$ . The Kapitza resistance can be modified by tuning either the liquid solid interaction coefficient  $c$ , or the mass density of the solid, or a combination of these two parameters. Figure 3 illustrates the variation of the measured effective conductivity for several values of the Kapitza resistance, determined independently for various values of these parameters. It is seen that the observed variation (decrease in our case) in the effective conductivity is very well described by the Maxwell-Garnett expression. This expression also allows us to understand why the heat conductivity does not vary in a perceptible manner for small volume fractions ( $\sim 2\%$ ), for which the predicted change would be less than 2%, within our statistical accuracy.

## B. Study of Collective Effects

Next we study a system of volume fraction 12% containing two nanoparticles in various configurations, in order to investigate the influence of collective effects. In order to model the influence of microscopic particle clustering we study two particles tethered by soft springs and forced to stay in “contact”, directly interacting with each other (fig. 4. We



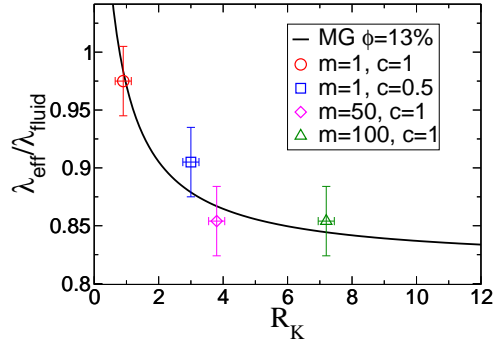


FIG. 3: Comparison between the ratio of the effective conductivity to the conductivity of the pure liquid of the simulated systems and the values obtained from the Maxwell Garnett equation.

modify the position of the centers of mass of the particles with respect to the temperature gradient - the particles are either aligned parallel or perpendicular to the gradient. In these two situations the solid phase has an aspect ratio of either  $a = 2$  (parallel) or  $a = 1/2$  (perpendicular). We also varied the Lennard-Jones interaction intensity between the two particles ( $\varepsilon_{pp}$ ) in order to increase the rate of particle-particle energy transfer. The particles-liquid thermal resistance is also modified by choosing different wetting properties or different ratios of the masses of the atoms belonging to the two phases. Finally, to explore a broader range of configurations, we also modified the distance between the centers of mass of the particles. In most configurations the particles are directly interacting with each other and in two setups they are separated along the  $z$  direction by a layer of atoms from the liquid phase, with a thickness of the order of a particle diameter. An overview of the systems investigated is shown in table II B.

First we study systems with aspect ratio  $a = 2$  and strong particle-particle interaction, as a function of the interfacial resistance with the fluid (fig. 4). The strong interaction is essentially equivalent to a chemical bonding between the particles. The two particles move as a single rigid body and the heat transfer between them is considerably enhanced. We can therefore reasonably compare the obtained conductivities with the values an effective medium calculation would predict for an ellipsoid with the same aspect ratio. A calculation including interfacial thermal resistance for ellipsoidal particles of the same

System name	Aspect ratio $a$	$\varepsilon_{pp}$	$m_p/m_l$	$c$	$R_K$	Particle-particle $\Delta r$
$a2\varepsilon1m1c1$	2.0	1.0	1	1	0.8	$2R_p$
$a2\varepsilon10m1c1$	2.0	10.0	1	1	0.8	$2R_p$
$a2\varepsilon1m50c1$	2.0	1.0	50	1	4.0	$2R_p$
$a2\varepsilon10m50c1$	2.0	10.0	50	1	4.0	$2R_p$
$a2\varepsilon10m1c0.5$	2.0	1.0	1	0.5	3.2	$2R_p$
$a0.5\varepsilon1m1c1$	0.5	1.0	1	1	0.8	$2R_p$
$a0.5\varepsilon10m1c1$	0.5	10.0	1	1	0.8	$2R_p$
$a0.5\varepsilon1m50c1$	0.5	1.0	50	1	4.0	$2R_p$
$a0.5\varepsilon10m50c1$	0.5	10.0	50	1	4.0	$2R_p$
$\varepsilon1m1c1$	$\times$	1.0	1	1	0.8	$4R_p$
$\varepsilon1m50c1$	$\times$	1.0	50	1	4.0	$4R_p$

TABLE I: Description of the systems containing two particles . The last column indicates the distance between the centers of mass of the two particles.

size, aligned with the thermal gradient, relevant for this situation can be derived from a general expression in ref.<sup>14</sup>. The ratio of the effective conductivity to the conductivity of the pure liquid is given by:

$$\frac{\lambda_{eff}}{\lambda_l} = \frac{1 + \Phi\beta(1 - L_{zz})}{1 - \Phi\beta L_{zz}} \quad (7)$$

where  $\Phi$  is the volume fraction,  $L_{zz}$  is given by

$$L_{zz} = 1 - 2 \left( \frac{a^2}{2(a^2 - 1)} - \frac{a^2}{2(a^2 - 1)^{3/2}} \cosh^{-1} a \right) \quad (8)$$

with aspect ratio  $a > 1$ . The parameter  $\beta$  is given by

$$\beta = \frac{\lambda^c - \lambda_l}{\lambda_l + L_{zz}(\lambda^c - \lambda_l)} \quad (9)$$

where

$$\lambda^c = \frac{\lambda_p}{1 + \frac{\lambda_p}{\lambda_l} (2 + 1/a) \frac{R_K \lambda_l}{R_p} L_{zz}} \quad (10)$$

In the above  $\lambda_p$  and  $\lambda_l$  are the conductivities of the particles and the liquid,  $R_p$  is the particles radius and  $R_K$  - the Kapitza resistance of the particle-liquid interface. The relations hold for an aspect ratio  $a > 1$ .

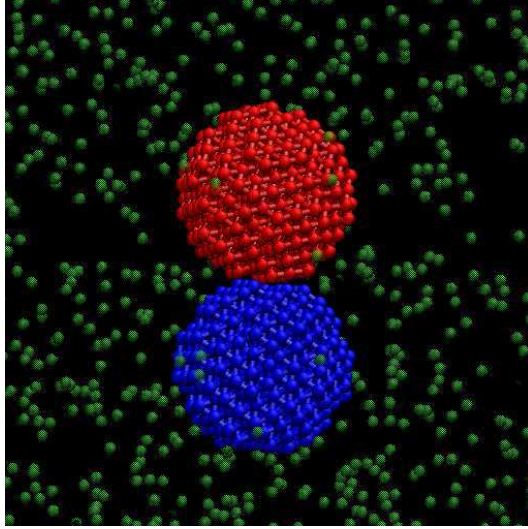


FIG. 4: Snapshot of the system containing two particles aligned with the temperature gradient having strong particle-particle interaction.

As can be seen in figure 5 the measured conductivities are in reasonable agreement with the calculation. For the smallest interfacial resistance there is an enhancement of the composite system conductivity by 5 to 10%. For larger values of  $R_K$  the small radius of the particles results in a decrease in the conductivity, due to interfacial effects.

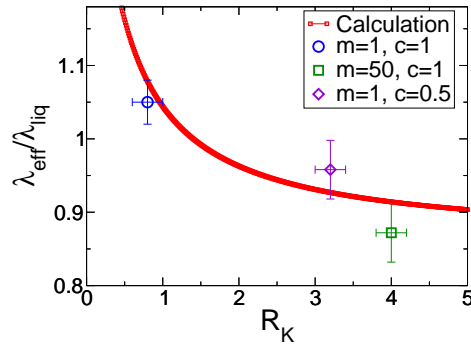


FIG. 5: Comparison of the measured variation in conductivity in the  $\varepsilon = 10$ ,  $a = 2$  systems to the prediction of the effective medium calculation with aspect ratio 2 and volume fraction 0.12 (equation 7).

Next, we study the thermal behavior of the systems with particles aligned with the

thermal gradient but much weaker interactions. The particle-particle interaction is taken to be neutral,  $\varepsilon_{pp} = 1$  (configurations  $a2\varepsilon1m50c1$ ,  $a2\varepsilon1m1c1$  in table II B). For this weaker interaction, we find that the conductivity is typically 4% below the one obtained with the strong attractive interaction. This difference can be understood from the temperature profiles shown in figure 6. The weaker interaction results in a higher resistivity in the "neck" region, at the boundary between the two particles. As the strongly attractive in-

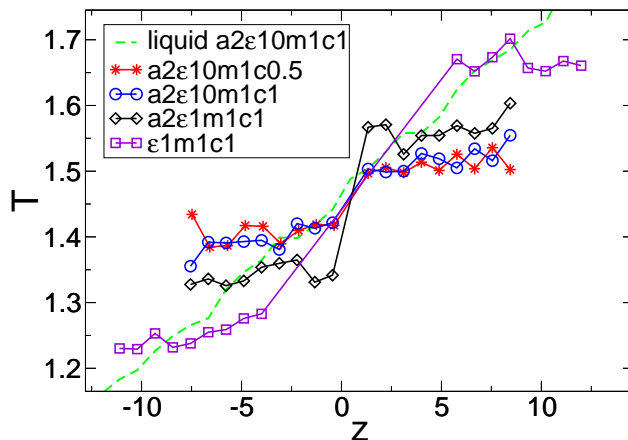


FIG. 6: Temperature profiles in the particles in the  $m = 1$  systems in stationary heat flow. The temperature profile within the liquid is also shown for one of the systems. For the other systems the liquid temperature profile is very similar. Stronger interaction decreases the temperature difference between the particles by approximately 50% compared to particles separated by the same distance with neutral interaction.

teraction decreases the particle-particle thermal resistance, the particles temperatures are closer for  $\varepsilon_{pp} = 10$ . As the particles are much more conductive than the liquid phase their temperature varies very little within their dimension. We observed that the temperature difference between the particles decreases by a factor of two when the interaction intensity is increased by a factor of ten:  $\Delta T = 0.22$  for  $\varepsilon_{pp} = 1$  and  $\Delta T = 0.12$  for  $\varepsilon_{pp} = 10$  in the systems of  $m = 1$ . In the  $m = 50$  case  $\Delta T(\varepsilon_{pp} = 1) = 0.44$  and  $\Delta T(\varepsilon_{pp} = 10) = 0.2$ . Because of the layers of fluid (of thickness around  $5\sigma$ ) remaining in both cases between the particles and the thermostats the global conductivity of the slab is still dominated by

interfacial effects and its increase is small.

When the particle-particle distance is increased, so that the particles do not interact directly with each other, the conductivity of the sample stays nearly identical (difference  $\sim 1\%$  in favor for the system where the particles are closer) to the case where they are in contact and with neutral interaction. Knowing that the contact area is very small when the particles are close and also given that the interaction is not strong, being equal to the interaction with the liquid atoms  $\varepsilon_{pp} = \varepsilon = 1$ , the inter particle distance in this case does not play an important role in the value of the conductivity. As can be seen in fig. 6, whenever  $\varepsilon_{pp} = \varepsilon = 1$  the average temperature of the particle is close to the average temperature of the liquid at the  $z$  coordinate of its center of mass, the particle thermalizes with the surrounding fluid. In contrast, when  $\varepsilon_{pp} = 10$  the inter particle heat flux becomes important and the two particles behave more like a single body.

We now turn to the conductivity of the systems where the particles are in the plane situated in the middle of the box and orthogonal to the temperature gradient. The heat fluxes measured for such systems of aspect ratio  $1/2$ , with strong and neutral particle-particle interaction, were identical within our statistical accuracy (difference less than one percent). The conductivities in this case are slightly lower, with about  $4.5\%$  ( $2\%$  for  $m = 1$  and  $7\%$  for  $m = 50$ ) than in the case where the particles are aligned with the temperature gradient and has neutral interactions ( $\varepsilon_{pp} = 1$ ). The difference is further increased to  $\sim 8\%$  ( $7\%$  for  $m = 1$  and  $10\%$  for  $m = 50$ ) when the  $a = 0.5$  systems are compared with the  $a = 2$  and  $\varepsilon_{pp} = 10$  systems.

In summary, we showed that the mutual positions of the particles in suspension in the fluid has an influence on the thermal conductivity of the system. If the particles interact so that clustering occurs in the suspension, the global conductivity of the nanofluid can increase to values higher than the one of a pure fluid, even if a well dispersed suspension at the same volume fraction has a conductivity lower than the pure system. The alignment with the temperature gradient enhances the conductivity and its effect on a microscopic level can be predicted by effective medium calculation taking into account the aspect ratio of the particle cluster. According to the effective medium prediction the ratio of the slab conductivity to the conductivity of the pure liquid grows essentially linearly with the

number of aligned particles (or the aspect ratio) (see fig. 7) when this number is smaller than the ratio of the conductivities of the two phases ( $\lambda_p/\lambda_l$ ). Hence even a moderate clustering (e.g. in strings of 3 to 4 particles) could be sufficient to interpret increases in the thermal conductivity compared to standard effective medium predictions.

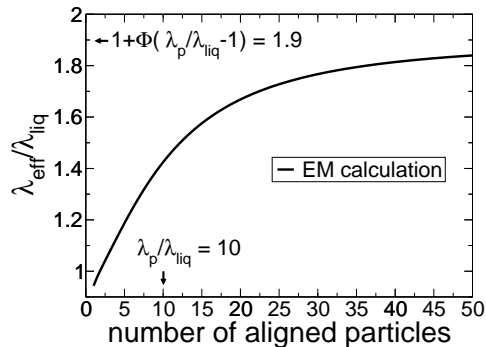


FIG. 7: Prediction of the effective medium calculation (equation 7) for the ratio of the system conductivity to the conductivity of the liquid for an interfacial resistance  $R_K = 1$ , a volume fraction  $\Phi = 0.1$ , and a ratio of 10 between the thermal conductivities of the solid and of the liquid. .

The enhancement tends to  $(1 - \Phi) + \Phi\lambda_p/\lambda_l$  when the aspect ratio tends to infinity. Thus, following this calculation that seems to give reasonable results at least on the scale of two particles and given that the ratio  $\lambda_p/\lambda_l$  is usually high in real nanofluids, a large enhancement can be expected if aggregates of particles are formed in the suspension. Our calculation concerns string like aggregates, but it is likely that similar effects would be observed with other types of aggregates, e.g. fractal ones with a low enough dimension.

### III. CONCLUSION

We have explored some aspects of the thermal properties of "nanofluids", at the level of model system, individual solid particles and collective effects involving two particles on a microscopic scale.

By varying interaction parameters or mass density, we are able to vary the interfacial

resistance between the particle and the fluid in a large range. This allowed us to estimate, over a large range of parameters, the effective heat conductivity of a model nanofluid in which the particles would be perfectly dispersed. The results for this setup can be simply explained in terms of the classical Maxwell-Garnett model, provided the interfacial resistance is taken into account. The essential parameter that influences the effective conductivity turns out to be the ratio between the Kapitza length and the particle radius, and for very small particles a decrease in conductivity compared to bulk fluids is found.

We also examined the effect of particle clustering and alignment with respect to the temperature gradient. We found that alignment improves the conductivity of the nanofluid in accordance with calculation with effective medium approach. Increased inter particle interaction further enhances conductivity. The results for small clusters of particles can again be described by effective medium theory, taking into account anisotropy and interface effects. Clustering of particles into string like objects is therefore suggested as a possible mechanism for obtaining larger conductivities, compared to the case of well dispersed suspensions.

In order to draw more precise conclusions concerning the conductivity dependence on the complex physics of collective effects larger systems containing more complex aggregates should be examined. The present study provides guidelines and outlines general tendencies that are to be expected in a larger and more complex system.

#### IV. APPENDIX

We present here a brief derivation of the Maxwell Garnett equation for the effective thermal conductivity in a two phase media (matrix with spherical inclusions) taking into account the interfacial thermal resistance. We consider a macroscopically homogeneous material with thermal conductivity  $\lambda_{eff}$  in a temperature gradient following some axis:  $T_{eff}(r) = -\mathbf{g} \cdot \mathbf{r}$ . We concentrate on a spherical inclusion of radius  $r_0$  and conductivity  $\lambda_1$  surrounded by a spherical shell of host material of thickness  $r_1$ , matrix conductivity  $\lambda_2$  and we assume that the inclusion does not change the temperature field for  $r > r_1$ . The two radii define the volume fraction of the inclusion,  $\Phi = r_0^3/r_1^3$  (fig. 8). The effective

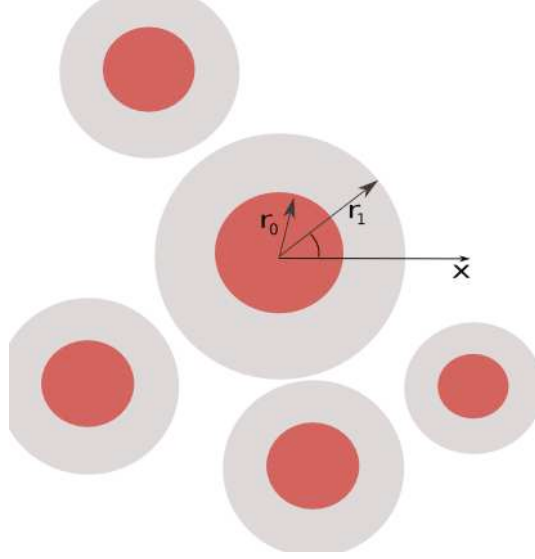


FIG. 8: Schematic presentation of the matrix with dispersed inclusions

conductivity can be determined by solving the steady state diffusion equation for the temperature:

$$\Delta T(r, \theta) = 0 \quad (11)$$

where  $\theta$  is the angle between  $\mathbf{r}$  and the external gradient  $\mathbf{g}$ . The solutions of equation 11 in the three different regions are given by:

$$T_1(r, \theta) = Ar \cos \theta, \quad 0 < r \leq r_0 \quad (12)$$

$$T_2(r, \theta) = (Br + E/r^2) \cos \theta, \quad r_0 < r \leq r_1 \quad (13)$$

$$T_{eff}(r, \theta) = -gr \cos \theta, \quad r_1 < r \quad (14)$$

The unknown constants in the equations above are to be determined from the appropriate boundary conditions. These are obtained by expressing the continuity of the heat flow at the domain boundaries and the value of the temperature field:

$$T_1(r_0, \theta) - T_2(r_0, \theta) = -\lambda_1 \frac{\partial T_1}{\partial r}(r_0) R_K \quad (15)$$

$$\lambda_1 \frac{\partial T_1}{\partial r}(r_0) = \lambda_2 \frac{\partial T_2}{\partial r}(r_0) \quad (16)$$

$$T_2(r_1, \theta) = T_{eff}(r_1, \theta) \quad (17)$$

$$\lambda_2 \frac{\partial T_2}{\partial r}(r_1) = \lambda_{eff} \frac{\partial T_{eff}}{\partial r}(r_1) \quad (18)$$



where  $R_K$  is the interfacial thermal resistance responsible for a temperature jump at the matrix-inclusion interface. Substituting the solutions for the temperature fields in equations 16-18, we end up with the following relations:

$$Ar_0^3 - Br_0^3 - E + \lambda_1 R_K Ar_0^2 = 0 \quad (19)$$

$$\lambda_1 Ar_0^3 - \lambda_2 Br_0^3 + 2\lambda_2 E = 0 \quad (20)$$

$$Br_1^3 + E + gr_1^3 = 0 \quad (21)$$

$$\lambda_2 Br_1^3 - 2\lambda_2 E + \lambda_{eff} gr_1^3 = 0 \quad (22)$$

Using this set of equations, one can obtain the Maxwell Garnett equation for the effective conductivity with interfacial thermal resistance:

$$\frac{\lambda_{eff}}{\lambda_2} = \frac{\left(\frac{\lambda_1}{\lambda_2}(1 + 2\alpha) + 2\right) + 2\Phi\left(\frac{\lambda_1}{\lambda_2}(1 - \alpha) - 1\right)}{\left(\frac{\lambda_1}{\lambda_2}(1 + 2\alpha) + 2\right) - \Phi\left(\frac{\lambda_1}{\lambda_2}(1 - \alpha) - 1\right)} \quad (23)$$

where  $\alpha = R_K \lambda_2 / r_0$ .

- 
1. Eastman, J. A.; Choi, S. U. S.; Li, S.; Yu, W.; Thompson, L. J.; *Appl. Phys. Lett.* **2001**, *78*, 718.
  2. Patel, H. E.; Das, S. K.; Sundararajan T.; Nair, A. S.; George, B.; Pradeep, T.; *Appl. Phys. Lett.* **2003**, *83*, 2931.
  3. Putnam, S. A.; Cahill, D. A.; Ash, B. J.; Schadler, L. S.; *J. Appl. Phys.*, **2003**, *94*, 6785.
  4. Keblinski, P.; Eastman, J. A.; Cahill, D. A.; *Materials Today*, **2005**, *8*, 36.
  5. Prasher, R.; Bhattacharya, P.; Phelan, P. E.; *Phys. Rev. Lett.* **2005**, *94*, 025901.
  6. Alder, B.J.; Wainwright, T.E.; *Phys. Rev. A*, **1970**, *1*, 18.
  7. Keblinski, P.; Thomon, J.; *Phys. Rev. E* **73**, 010502 (2006)
  8. Keblinski, P.; Phillot, S. R.; Choi, S. U.-S.; Eastman, J. A.; *Int. J. of Heat and Mass Transf.* **2002**, *45*, 855.
  9. Putnam, S. A.; Cahill, D. G.; P. V. Braun, P. V.; Ge, Z.; Shimmin R. G.; *J. Appl. Phys.*, in press
  10. Vladkov, M.; Barrat, J.-L.; *Nanolett.*, **2006**, *6*, 1224 (2006)

11. Evans, W.; Fish, J.; Koblinski, P.; *Appl. Phys. Lett.*, **2006**, *88*, 093116.
12. Barrat, J.-L.; Bocquet, L.; *Faraday Discussions* **1999**, *112*, 121.
13. Barrat, J.-L.; Chiaruttini, F.; *Molecular Physics* **2003**, *101*, 1605.
14. Nan, C. W.; Birringer, R.; Clarke, D. R.; Gleiter, H.; *J. Appl. Phys.*, **1997**, *81*, 6692.